



# Maximal Heights of Nearshore Storm Waves and Resultant Onshore Flow Velocities

Nans Bujan<sup>1\*†</sup> and Rónadh Cox<sup>2,3\*</sup>

<sup>1</sup> International Wave Dynamics Research Center, National Cheng Kung University, Tainan, Taiwan, <sup>2</sup> Geosciences Department, Williams College, Williamstown, MA, United States, <sup>3</sup> School of Earth Sciences, University College Dublin, Belfield, Ireland

## OPEN ACCESS

### Edited by:

Juan Jose Munoz-Perez,  
University of Cádiz, Spain

### Reviewed by:

Pedro J. M. Costa,  
University of Coimbra, Portugal  
A. B. M. Khan Mozahedy,  
Bangladesh Water Development  
Board (BWDB), Bangladesh

### \*Correspondence:

Nans Bujan  
n-bujan@yandex.com  
Rónadh Cox  
rcox@williams.edu

### † Present address:

Nans Bujan,  
Wildlands Studies, Aptos, CA,  
United States

### Specialty section:

This article was submitted to  
Coastal Ocean Processes,  
a section of the journal  
Frontiers in Marine Science

Received: 27 December 2019

Accepted: 16 April 2020

Published: 03 June 2020

### Citation:

Bujan N and Cox R (2020) Maximal Heights of Nearshore Storm Waves and Resultant Onshore Flow Velocities. *Front. Mar. Sci.* 7:309. doi: 10.3389/fmars.2020.00309

Storm waves, after breaking or overtopping, generate strong onshore flows that do significant mechanical work, including eroding and transporting large boulders. The waves can be amplified on approach, and the flows themselves may be further intensified by local topographic effects. These processes are currently poorly parameterised, but are of great importance for understanding the interactions between waves and coasts. We present a highly generalised equation for estimating maximal coastal wave heights and consequent onshore flow velocities. Although very approximate, this method contains no embedded assumptions, and thus provides a more realistic first-order check of storm wave capabilities than previous approaches. Initial analysis suggests that exceptional wave impacts may generate onshore flow velocities up to six times greater than expected from previous approaches. Although the probability of occurrence in any given storm is very low, the possibility of such extreme values cannot be ignored, especially when interpreting ancient deposits of large boulders. The equations presented here can be used as a first-order test for coastal boulder deposits currently interpreted as tsunami deposits, to evaluate whether a storm-wave origin should be reconsidered. This approach could also be employed at coasts in general, to evaluate long-term probabilities of damaging flows, as a component of coastal risk analysis.

**Keywords:** boulders, tsunamis, waves, run-up, storms, cliffs, deposits, risk

## INTRODUCTION

The behaviour of large waves as they approach steep coasts is one of the great unknowns in marine science. In contrast to waves that shoal gradually across smooth bathymetry, and run up gentle slopes—which are well-described and amenable to mathematical modelling—waves at rocky coasts are far less studied. They are difficult to measure, and equally difficult to model (Dodet et al., 2018; Herterich and Dias, 2019). Thus, there are few data for storm-wave runup in those environments. This matters, because coastal wave energy fluxes are predicted to increase (Mentaschi et al., 2017) and reliable risk analysis for coastal populations is urgently needed (e.g., Switzer et al., 2014; Esteban et al., 2016; Breivik et al., 2017). It is therefore important to understand inshore transmission of storm-wave energy. Extreme wave behaviour can most readily be observed at exposed rocky coasts.

Coastal boulder deposits have received attention as markers for extreme wave inundation events (e.g., Nott, 2003a; Lorang, 2011; Cox et al., 2018). However, there has been controversy about the kinds of power required to emplace supratidal megagravel, i.e., boulders with an intermediate axis

longer than 4.1 m (e.g., Switzer and Burston, 2010; Engel and May, 2012; Kennedy et al., 2016; Weiss and Sheremet, 2017). Some workers argue that storm waves are insufficiently powerful to move massive boulders, which are therefore often interpreted to be tsunami deposits (Scicchitano et al., 2007; Scheffers and Kinis, 2014; Roig-Munar et al., 2019a). But abundant recent evidence shows that storm waves can and do move extremely large rocks (e.g., May et al., 2015; Kennedy et al., 2017; Cox et al., 2018; Cox, 2019). New applications of surface-exposure dating to coastal boulders are revealing chronologies that conflict with tsunami interpretations (e.g. Brill et al., 2020), and new models of responses to wave loading are revealing the true power of storms (e.g., Park et al., 2018). Thus, parameterising wave and flow amplification at steep coasts can help close the interpretive gap for coastal boulder deposits, and also provide a framework for coastal risk analysis.

Previous attempts to calculate coastal wave heights have employed a hindcasting method, using masses of emplaced boulders to calculate the minimum flow velocity and thence wave height needed to transport them (Nott, 2003b; Pignatelli et al., 2009; Barbano et al., 2010; Benner et al., 2010; Engel and May, 2012; Mottershead et al., 2014). This approach however, embeds preconceptions about onshore flow hydrodynamics, relying on the presumption of a fixed Froude number depending on wave type (Kennedy et al., 2016; Cox et al., 2020).

Here, we take a different tack. Examining factors that contribute to wave height amplification and onshore bore velocity, we estimate maximal onshore wave impacts that might occur, given offshore significant wave height  $H_s$ . These estimates can be compared to existing boulder masses, but do not depend on them; and further, can be applied to structural design specifications at any coastline. Extreme waves and flow velocities are low-probability events, but appraising their impacts provides an additional lens for examining coastal boulder deposits, and also long term potential for storm damage at coasts.

## ESTIMATING COASTAL WAVE-HEIGHT MAXIMA

Approaching the shore, waves interact with other waves, sea-bottom topography, and coastal geometry. Many waves are dampened, others amplified—sometimes tremendously (Herterich and Dias, 2019). The highest possible coastal wave-crest elevation will occur if the largest wave in a sea undergoes maximum amplification during shoaling and runup. Clearly, this will be a rare occurrence, with very low probability in any given storm. Over many storms, however the likelihood increases. Thus, in long-term evaluations of coastal change or coastal risk, maximal events should not be ignored.

Coastal wave heights depend on complex interplay of surface water with wind gust and fetch, as well as interactions with bathymetry and topography. The maximum offshore wave height  $H_{max}$  can be approximated by  $2H_s$  (e.g., Krogstad, 1985; Cattrell et al., 2018), but seas evolve as they transit the shelf and shoal toward land, so that  $H_{max}$  obtained from buoy data may not match maximum wave height at the coast. Wave energy attenuates across the continental shelf, typically causing large

swell height to decrease by about half (Ardhuin et al., 2003; Janjić et al., 2018), but amplification commonly occurs near shore, as shoaling waves interact with sea bed and coast (Viotti and Dias, 2014; Akrish et al., 2016; Brennan et al., 2017). Predicting coastal wave heights is therefore complicated.

Here we consider only pre-impact unbroken waves, and horizontal inland bore velocity. We ignore storm surge, tide level, and infragravity effects, which for this analysis represent short-term sea-level increases. In particular too, we ignore jetting, by which waves impacting cliffs can generate spray heights far greater than the incident wave height (e.g., Peregrine, 2003; Lugni et al., 2006). Although important for erosion (e.g., Bredmose et al., 2015), and for quarrying cliff-top boulders (e.g., Herterich et al., 2018), most of that force is directed vertically. Part of the jet may collapse on the cliff-top platform, but with relatively little inshore transmission of mass or energy. Horizontal flows generated by breaking or overtopping waves are the main agents of onshore sediment movement and structural damage; and our analysis therefore focuses on waves likely to produce them.

## Factors Contributing to Wave Height at the Coast

Processes affecting incoming waves can be given as variables in an expression relating offshore  $H_s$  to the crest elevation of the largest wave impacting the coast  $\eta_{max}$ :

$$\eta_{max} = C_{max}C_{atten}C_{amp}H_s \quad (1)$$

$C_{max}$  is the multiplier relating  $H_{max}$  to  $H_s$  ( $H_{max} = C_{max}H_s$ ), and has a value  $\geq 1$  ( $H_{max}$  being either measured or statistically inferred).  $C_{atten}$  describes the proportional attenuation as waves cross the continental shelf, and thus has a maximum value of 1.  $C_{amp}$  describes nearshore amplification, as shoaling waves interact with bathymetry. Because  $\eta_{max}$  is the sea surface elevation above still-water level (i.e. not crest-trough height), then in the case where there is no amplification relative to  $H_s$ ,  $C_{amp} = 0.5$  (i.e.,  $\eta_{max}$  is given by local amplitude, or half the inshore wave height). Values  $> 0.5$  denote increasing amplification.  $C_{amp} = 1$  would be the case where sea surface elevation is at double the amplitude of the incoming wave before amplification. We discuss and quantify each of these variables below.

Theoretically, as outlined above,  $C_{max} \sim 2$  (because  $H_{max} \sim 2H_s$ ); and  $C_{atten} \sim 0.5$ . At first blush, therefore, the two factors cancel, suggesting that offshore  $H_s$  may be a reasonable predictor of the upper end of the coastal wave height spectrum. But we emphasise that this will vary. If, for example,  $H_s$  data come from an inshore buoy, or the continental shelf is narrow, there will be little attenuation, so for our illustration we choose  $C_{max} = 2$  and  $C_{atten} = 1$ .

Choosing a value for  $C_{amp}$  is difficult, because complexities abound near the coast (Hansom et al., 2008; Didenkulova and Pelinovsky, 2011; Slunyaev et al., 2011; Carbone et al., 2013). Reflection can double wave height by simple constructive interference ( $C_{amp} = 1$ ); but non-linear interactions, and complex interplay with irregular bathymetry and other waves,



**FIGURE 1** | Strongly amplified wave overtopping the harbour wall at Kalk Bay, Cape Town, South Africa, on June 3rd, 2015. The greatest  $H_s$  offshore of Cape Town on that day was  $\sim 4\text{--}5$  m (South African Weather Service, document reference: ops-fcast-CT-083). The lighthouse is 6 m tall; the continuous green-water wall is almost 12 m high, i.e., more than twice the offshore  $H_s$ . Photo copyright Rob Tarr (<https://www.sapeople.com/2015/07/11/massive-waves-south-africa-kalk-bay-harbour-waves/>), used with permission.

can add even greater amplification. Modelling shows that runup elevations may reach several times the off-shore wave height (Akrish et al., 2016; Brennan et al., 2017; Herterich and Dias, 2017a,b, 2019).

Here, we adopt a conservative value of  $C_{amp} = 1$ , based on numerous measurements of inshore waves  $> 2H_s$  (i.e., “rogue waves,” e.g., Kharif and Pelinovsky, 2003; Gemmrich and Thomson, 2017). Photographs document dramatic amplifications for which there are no direct measurements, but which are clearly exceptional waves of substantial size (e.g., **Figure 1**). In some places and at some times—e.g., locations with unusual topography, providing resonances with certain wave spectra (e.g., Brennan et al., 2017; Herterich and Dias, 2019)— $C_{amp}$  may be  $> 1$  (e.g., Didenkulova et al., 2006; Didenkulova and Anderson, 2010). At most sites, however, it should be less. And we emphasise that users should pick coefficient values appropriate for individual sites.

### Overtopping Wave Height: Taking Coastal Elevation Into Account

At sea level,  $\eta_{max}$  fully describes impinging wave amplitude. At steep or cliffed coasts, however, only the overtopping portion of the wave will propagate inland (**Figure 2**). Therefore,

coastal elevation  $Z$  must be subtracted from  $\eta_{max}$  to calculate overtopping wave height  $h_O$ :

$$h_O = \eta_{max} - Z = C_{max}C_{atten}C_{amp}H_s - Z \quad (2)$$

On low-lying shores,  $Z \sim 0$  so that  $h_O$  is essentially  $\eta_{max}$ , and the full height of the wave comes ashore to generate the overland bore. Where there is a cliff or a seawall,  $Z$  is the elevation of that barrier. If the coast is steeply sloping but not vertical, the simplest approach is to use the elevation at the point of interest: e.g., in the case of boulder movement or infrastructure impact,  $Z$  is the elevation at that location. We do not apply any correction for energy dissipation as water moves inland and against gravity, but such calculations exist (e.g., Noormets et al., 2004; Ogawa et al., 2015; Poate et al., 2018), and can be incorporated into these equations.

### ESTIMATING MAXIMUM BORE VELOCITY ONSHORE

Onshore flow takes many forms, including swash uprush following breaking and dryland bores formed by collapse of overtopping waves (**Figure 2**). The processes are complex,



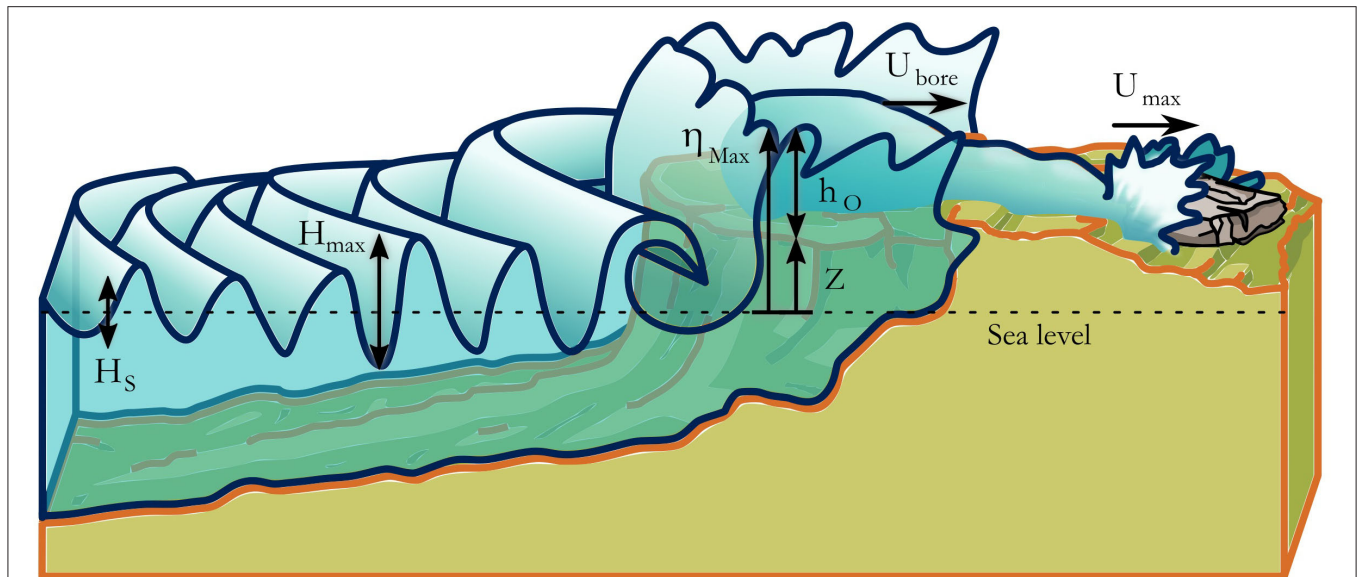


**FIGURE 2** | Highly stylised diagram of wave amplification and flow acceleration at the coast. This is not intended as a realistic depiction of a wave storm sea, but simply illustrates components discussed in the text. Offshore wave spectra can include large individual waves ( $H_{max}$ ). Interaction with bathymetry and with steep coastal topography may further amplify the largest waves, resulting in an extreme surface elevation at the coast  $\eta_{max}$ , with the elevation above the land surface given by  $h_0$ . Collapse on the coastal platform or cliff top yields a bore with velocity  $U_{bore}$ , which may be focussed and accelerated by topography, generating high-energy flows ( $U_{max}$ ) with the capability of moving large boulders.

multiphase, and difficult to model, but field and lab observations show that storm waves can generate flows hydrodynamically similar to tsunami bores (Kennedy et al., 2016; Wüthrich et al., 2018).

Dam-break theory (Ritter, 1892) relates horizontal velocity of the bore front  $U_{bore}$  to wave height  $H$ :

$$U_{bore} = C_{dam} \sqrt{gH} \quad (3)$$

For a horizontal dry bed, analytical solutions give  $C_{dam} = 2$  (Ritter, 1892; Chanson, 2006), but experiments and measurements show that the value actually varies considerably in natural settings (Chanson, 2006; Hansom et al., 2008; Hu et al., 2015). This makes sense, because hydrodynamically,  $C_{dam}$  is simply the Froude number  $Fr$ <sup>1</sup>. Wave-generated flows can have  $Fr > 2$  (Holland et al., 1991; Hansom et al., 2008) and even  $Fr \geq 4$  (Matias et al., 2016). Likewise, tsunami flows with lower  $Fr (< 2)$  are also common (e.g., Yeh, 1991; Imamura et al., 2008; Matsutomi and Okamoto, 2010). We therefore cast  $C_{dam}$  as a variable ( $> 0$ ), with value depending on local topographic and roughness conditions.

We can restate the Ritter equation in terms of Equation (2):

$$U_{bore} = C_{dam} \sqrt{gh_0} \quad (4)$$

where  $U_{bore}$  is onshore flow velocity, and  $h_0$  can be thought of as the instantaneous depth of water above the shore platform (e.g., Hu et al., 2015).

<sup>1</sup>Since  $Fr = \frac{U}{\sqrt{gD}}$  where  $D$  is the depth of the flow.

## Factors that Amplify Flow Velocity

Variability in real-world bore velocities is substantially greater than predicted by classic dam-break theory. Lab and field measurements in many environments—from overwash of sandy and gravel barriers to greenwater overtopping of platforms—have yielded  $C_{dam}$ -equivalent values ranging from 1.2 to 10 (Holland et al., 1991; Cox and Ortega, 2002; Ryu et al., 2007; Donnelly, 2008; Chang et al., 2011; Matias et al., 2014, 2016; Chuang et al., 2015; Song et al., 2015; Wüthrich et al., 2018). These coefficients are both higher and lower than the theoretical Ritter (1892) value of 2. Environmental interactions clearly regulate flow behaviour, sometimes weakening but often accelerating it.

A major mechanism for flow-front acceleration, commonly overlooked, is topographic focusing after wave-breaking and during bore propagation (Denny et al., 2003). This funneling and acceleration can be expressed by a parameter  $C_{topo} (\geq 1)$ , yielding an expression for maximum onshore velocity:

$$U_{max} = C_{topo} U_{bore} \quad (5)$$

Which can be restated as:

$$U_{max} = C_{topo} C_{dam} \sqrt{gh_0} \quad (6)$$

$C_{topo}$  is difficult to estimate, and data for surf-zone flow velocities under high-energy conditions are rare. But the few measurements available indicate that strong flow magnifications do occur during runup on uneven rocky coasts. For example, Yeh et al. (1994) reported that convergence of refracted wave fronts produced a three-fold increase in tsunami bore runup velocity.

Denny et al. (2003) showed that collision of refracted bore fronts, channeled and focused by topography, can double flow speeds, i.e.,  $C_{topo} = 2$ . Similarly, Carrasco et al. (2014), studying a breakwater with large roughness elements, reported overtopping flows with  $U_{max}$  of 11 m/s, related to 5 m waves. Plugged into Equation (6) and assuming  $C_{dam} = 2$ , this yields  $C_{topo} \sim 4.5$ . These are only two studies, and without more data it's hard to know how representative they are; but whereas the Carrasco et al. (2014) study was short term and at one location, the Denny et al. (2003) study encompassed a 1.5-year time series of field data from 221 sites, backed up with wave tank experiments, both approaches yielding velocity-amplification factors  $\sim 2$ . Recognising that Denny et al. (2003) may not have captured the maximum possible amplification, and pointing out that more studies of this phenomenon are needed, we choose  $C_{topo} = 2$  as a reasonable preliminary value.

## A UNIFIED EQUATION RELATING OFFSHORE WAVE HEIGHT AND ONSHORE FLOW VELOCITY

Combining Equations (2) and (6), we can relate  $U_{max}$  to  $H_s$  to give a theoretical maximum velocity for wave-induced onshore flow:

$$U_{max} = C_{topo} C_{dam} \sqrt{g(C_{max} C_{atten} C_{amp} H_s - Z)} \quad (7)$$

With coefficient values as chosen above ( $C_{topo} = 2$ ,  $C_{dam} = 2$ ,  $C_{max} = 2$ ,  $C_{atten} = 1$ ,  $C_{amp} = 1$ ) and for locations at sea level ( $Z = 0$ ), Equation (7) becomes:

$$U_{max} = 2 \times 2 \sqrt{g(2 \times 1 \times H_s - 0)} = 4\sqrt{2gH_s} \sim 5.7\sqrt{gH_s} \quad (8)$$

Equation (8) means that for a given  $H_s$ —and if all amplification factors are maximised—resultant extreme onshore velocity could be almost six times that of a shallow-water wave with speed  $\sqrt{gH_s}$ . Such values deliberately push the envelope of what is possible and we emphasise that velocities this high relative to the generating wave heights would be exceedingly rare.

## COMPARISON WITH PREVIOUS APPROACHES

Previous studies calculating onshore flow velocities have generally used them to hindcast nominal heights for the bore-generating waves. The most widely applied approach in coastal boulder studies is that of Nott (1997, 2003b), which has driven thinking about likely heights and transport capacities of coastal wave flows (see Kennedy et al., 2019, their Table 1), so we address it in detail here.

Attempting to discriminate between tsunami and storm waves as mechanisms of boulder transport, Nott (1997, 2003b) introduced hydrodynamic equations linking clast characteristics to threshold horizontal flow velocity  $U_{bore}$ . Starting with boulder dimensions and density, he derived by force balance the flow velocity necessary for transport. Once this velocity is calculated,

the dam-break expression (Equation 3) can be reorganised and used to solve for wave height  $H$ —but only if the value of  $C_{dam}$  is known. Nott (2003b) assumed that the Ritter coefficient  $C_{dam} = 2$  would apply to all tsunami flows, and that flows generated by storm waves would have the velocity of a shallow water wave (i.e.,  $C_{dam} = 1$ ). He therefore defined a ‘wave parameter’  $\delta$  (equivalent to the square of the coefficient in the Ritter equation, or  $C_{dam}^2$  in the terminology of Equation 3). Thus, Nott’s (2003b) formulation for wave height is:

$$H = \frac{U_{bore}^2}{\delta g} \quad (9)$$

Nott’s presumption of specific  $\delta$  values (1 for storm waves and 4 for tsunami) opened a door to using boulder measurements to calculate nominal wave heights required for transport, with modifications for different pre-transport settings (i.e., whether the boulder was initially submerged, sitting on dry land, or still part of bedrock). Subsequent studies incorporated Nott’s (1997; 2003b) approach in a range of equations attempting to relate flow speeds to wave heights (see Table 1). Such equations are now often employed to hindcast wave heights for both modern and ancient coastal boulder deposits. In particular, they have frequently been used to argue that coastal boulders could not have been emplaced by storm waves, because the equations call for waves too large relative to measured or inferred  $H_s$  (e.g., Kennedy et al., 2007; Mastronuzzi et al., 2007; Scicchitano et al., 2007; Barbano et al., 2010; Boulton and Whitworth, 2017; Roig-Munar et al., 2019b).

Flaws in the Nott equations have been detailed by many (see Cox et al., 2020 and references therein). A key problem is that Nott’s (2003) wave parameter  $\delta$  is actually equivalent to  $Fr^2$  (Kennedy et al., 2016; Cox et al., 2020): Nott’s approach requires  $Fr = 1$  for storm waves and  $Fr = 2$  for tsunami, unvarying. But given the complexity of wave-coast interactions, and the non-linearity of wave breaking and overtopping (Cooker and Peregrine, 1992; Carbone et al., 2013), there is no basis for assuming that storm-wave flows have lower  $Fr$  than tsunami. Nott’s  $\delta$  is not a constant, but a variable, which will differ from one wave-generated flow to another. Therefore, Equation’s (9) central premise fails. In particular Nott’s (1997; 2003b) assumption that storm-wave bore velocity never exceeds shallow-water wave speed—hard-wired into the equations in Table 1—neglects local effects (and is contradicted by many observations, discussed previously). Thus, coastal storm-wave heights and flow velocities calculated by equations based on the Nott assumptions are not meaningful.

In contrast, the relationships laid out in Equation (7) are explicitly variable, and make no assumptions about hydrodynamic state. No coefficient values are stipulated. The equation is designed to be flexible and adaptable, providing an estimate of the most extreme conditions possible for a given storm and coastal setting.

## USES OF THESE EQUATIONS

This analysis indicates that storm waves can generate flows with  $\delta$ -equivalent values larger than those asserted in the

**TABLE 1** | Examples of existing formulations for minimum flow velocity and wave height required to displace a boulder.

Source	Pre-transport boulder setting	Expression for threshold flow velocity $U_{bore}$	Expression for threshold wave height $Min. H$
Nott (2003b)	Submerged	$\sqrt{\frac{2ag(\rho_s - \rho_w)/\rho_w}{C_d(ac/b^2) + C_L}}$	$\frac{2a(\rho_s - \rho_w)/\rho_w}{\delta(C_d(ac/b^2) + C_L)}$
Nott (2003b)	Subaerial	$\sqrt{\frac{2ag(\rho_s - \rho_w)/\rho_w - 4C_m\ddot{u}a/b}{C_d(ac/b^2) + C_L}}$	$\frac{2a(\rho_s - \rho_w)/\rho_w - 4C_m\ddot{u}a/(bg)}{\delta(C_d(ac/b^2) + C_L)}$
Nott (2003b)	Joint-bounded	$\sqrt{\frac{ag(\rho_s - \rho_w)/\rho_w}{C_L}}$	$\frac{a(\rho_s - \rho_w)/\rho_w}{\delta C_L}$
Pignatelli et al. (2009)	Joint-bounded	$\sqrt{\frac{2cg(\rho_s - \rho_w)/\rho_w}{C_L}}$	$\frac{2c(\rho_s - \rho_w)/\rho_w}{\delta C_L}$
Barbano et al. (2010)	Submerged	$\sqrt{\frac{2b^2cg(\rho_s - \rho_w)/\rho_w}{C_d c^2 + C_L b^2}}$	$\frac{2b^2c(\rho_s - \rho_w)/\rho_w}{\delta(C_d c^2 + C_L b^2)}$
Benner et al. (2010)	Submerged and subaerial	$\sqrt{\frac{2bc(bg(\rho_s - \rho_w)/\rho_w - C_m\ddot{u}c\rho_s/\rho_w)}{C_d c^2 + C_L b^2}}$	$\frac{2bc(bg(\rho_s - \rho_w)/\rho_w - C_m\ddot{u}c\rho_s/\rho_w)}{\delta g(C_d c^2 + C_L b^2)}$
Nandasena et al. (2011)	Joint-bounded	$\sqrt{\frac{2gc(\cos\theta + \mu \sin\theta)(\rho_s - \rho_w)/\rho_w}{C_L}}$	$\frac{V(\cos\theta + \mu \sin\theta)(\rho_s - \rho_w)/\rho_w}{0.5\delta C_L abQg}$
Engel and May (2012)	Joint-bounded	$\sqrt{\frac{V(\cos\theta + \mu \sin\theta)(\rho_s - \rho_w)/\rho_w}{0.5C_L abQ}}$	$\frac{V(\cos\theta + \mu \sin\theta)(\rho_s - \rho_w)/\rho_w}{0.5\delta C_L abQg}$

The threshold flow speed  $U_{bore}$  is calculated from boulder dimensions and then linked to a minimum wave height necessary for boulder transport  $Min. H$  through the relation  $Min. H = U_{bore}^2/(\delta g)$ . Equation terms are  $\delta$ , wave parameter (see text for explanations);  $a, b, c$ , long, intermediate, and short boulder dimensions;  $V$ , volume;  $\rho_s$ , boulder density;  $\rho_w$ , water density;  $\ddot{u}$ , instantaneous flow acceleration;  $C_d$ , drag coefficient;  $C_L$ , lift coefficient;  $C_m$ , inertia coefficient;  $\mu$ , static friction coefficient;  $Q$ , empirical coefficient;  $g$ , gravity;  $\theta$ , angle of the bed slope.

**TABLE 2** | Examples from the literature of large boulders, currently interpreted as tsunami-transported (based on application of equations similar to those of **Table 1**), but which may actually have been moved by storm waves.

Location	Data source	Boulder Mass W (t)	Z (m)	Motion threshold given in data source		Max. $H_s$ (m)	$U_{max}$ from Equation (7) (m/s)
				$U_{bore}$ (m/s)	Min. $H$ (m)		
Sicily, Italy	Scicchitano et al. (2007)	182	5	22	49.5	9.4	25.7
Apulia, Italy	Pignatelli et al. (2009)	74	4	20.9	44.4	7	21.5
Sicily, Italy	Barbano et al. (2010)	27	4	11.8	14.1	6.2	18.9
Makran, Iran	Shah-hosseini et al. (2011)	18	5	12.1	15	9.4	25.7
Maltese islands, Malta	Mottershead et al. (2014)	20	6.1	12.9	17	9	22
Crete, Greece	Boulton and Whitworth (2017)	691	2	12	12.7	5.5	22.2
Minorca, Spain	Roig-Munar et al. (2018)	229	6.8	21.3	46.3	11	25.8

$W$ , weight of heaviest boulder in study;  $Z$ , boulder elevation;  $U_{bore}$ , velocity threshold for boulder motion;  $Min. H$ , nominal minimum storm wave height required ( $Min. H = U_{bore}^2/g$ ), from the cited study;  $Max. H_s$ , largest  $H_s$  at the boulder location (used as nominal maximum wave height in the cited study);  $U_{max}$ , bore velocity calculated from Equation (7). Storm-wave transport was discounted in these studies because their calculated  $Min. H$  was greater than the known  $Max. H_s$ . However, applying Equation (7), with boulder elevations and  $Max. H_s$  from the cited studies (and using non-maximal coefficients: see text for details), shows that bores with sufficient velocity to move coastal megagravel ( $U_{max} \geq U_{bore}$ ) can be produced by storm waves consistent with local wave climate.

Nott Approach. For example, if  $H_s = 10$  m (i.e., conditions seen on sub-decadal timescales on high-energy coasts: e.g., Komar and Allan, 2007; Chen and Curcic, 2016; Masselink et al., 2016) an extreme onshore velocity  $U_{max}$  could be as great as 56 m/s according to Equation (8). This is more than 5 times the Nott  $U_{bore}$  corresponding value of 10 m/s, and would imply a  $\delta$ -equivalent value of 10 (i.e., ten times the Nott-asserted storm-wave value for  $\delta$ ).

It's extremely unlikely that all factors of Equation (7) would be maximized for any single wave event, and we do not imply that flows with outsize velocities occur during any given storm. But it is probable that some of these factors act on some large waves on a fairly regular basis, producing local runup velocities much greater than simple dam-break theory would predict. Didenkulova et al. (2006) reported that coastal waves with  $H \geq 2H_s$  occur much

more frequently than they are observed. We suggest that large coastal wave events and consequent high-velocity onshore flows occur more commonly than predicted from classical theories.

For illustration, we examined coastal boulders that have been interpreted as tsunami deposits via the argument that storm waves had insufficient power to move them. **Table 2** lists examples of such boulders from the literature, along with computed threshold velocities and upper limits on available wave energy. We used the published data (boulder dimensions, elevations, and wave climate information) as inputs for Equation (7), but we dialled down its coefficient values: we supposed waves that are 20% attenuated ( $C_{atten} = 0.8$ ), where  $H_{max}$  is 80% greater than  $H_s$  ( $C_{max} = 1.8$ ), and amplification occurs in the nearshore environment ( $C_{amp} = 0.8$ ). We also assumed that the resulting flow behaved like a classic dam break flow ( $C_{dam} = 2$ )

and could be accelerated 70% by topographic focusing ( $C_{topo} = 1.7$ ). The point of **Table 2** is to show that when amplification factors are considered—even if they are sub-maximal—bores potentially generated by storm waves are more than sufficient to move very large objects. Does this mean that storm waves have moved those boulders? Maybe, although that cannot be proved without additional evidence. The main result, however, is that the possibility of displacement by storm waves cannot be discarded on the basis of hydrodynamic equations alone. Any large storm wave can be rendered exceptional if the amplification factors align constructively.

As another illustration, let us consider the case of the largest boulder known to have been moved by storm waves (620 t, at 3 m above high water: Cox et al., 2018). Bore velocity required to slide this rock is around 11 m/s from equations in Nandasena et al. (2011) (velocity equations of Nott, 2003b return a higher value,  $\sim 17$  m/s, but do not adequately consider boulder geometry). The maximum  $H_s$  in the winter that this boulder moved was 14.7 m (Cox et al., 2018) but the Nott approach would require wave heights more than twice this. Boulders of this size (as well as smaller ones) are routinely interpreted as tsunami transported. However, per Equation (7), this boulder could have been moved by a wave with a height equivalent to  $H_s = 14.7$  m ( $C_{atten} = 1$ ,  $C_{max} = 1$ ,  $C_{amp} = 0.5$ ) and which produced a dam-break-style flow ( $C_{dam} = 2$ ) that had no topographic focusing ( $C_{topo} = 1$ ). Moreover, it could also have been moved by a much smaller wave, say  $\sim 10$  m on approach to the coast ( $C_{atten} = 0.5$ ,  $C_{max} = 1.4$ ), that was amplified inshore by 50% ( $C_{amp} = 0.75$ ), and then collapsed to form a dam-break flow ( $C_{dam} = 2$ ) that was mildly topographically focused ( $C_{topo} = 1.5$ ). Many other numerical combinations are possible, and we cannot know which ones may have occurred. But the point is that there are abundant ways to amplify storm waves sufficiently to produce bores strong enough to do extreme hydrodynamic work onshore.

We emphasize that the equations developed here are highly generalised and return indicator values only. They use a simple linear augmentation of height and velocity, whereas non-linear interactions certainly happen: non-linearity could yield extreme dampening, or additional amplification. The coefficients can only be approximate, because it is not possible to better constrain them. Despite recent advances in modelling (e.g., Weiss and Diplas, 2015; Zainali and Weiss, 2015; Zhang et al., 2017), the dynamics of high-energy coasts still are so poorly known that rough guesses are the best we can do. But coupled with reliable hydrodynamic estimates of the velocity required to move a boulder, this approach permits evaluation of wave conditions needed for transport. Given  $H_s$ , for example, one could use Equation (7) to estimate the combined total of the amplification factors required to match a threshold boulder-entertainment velocity. This would permit initial evaluation of the feasibility or likelihood of storm-wave transportation.

Exceptional events cannot be ignored when considering long-term storm histories, or future projections. Equations (2) and (6) provide a simple way to evaluate the kinds of amplifications that could generate remarkably large waves and accelerated bores. The longer the time period under consideration, the more important it is to consider the possibility that maximal waves might have

occurred. In the case of coastal boulder deposits, the timescale is commonly centuries to millennia (e.g., Barbano et al., 2010; Costa et al., 2011; Shah-hosseini et al., 2013; Rixhon et al., 2018), and it is generally decades to centuries in forward-looking risk analyses for coasts. It takes only one extraordinary wave to move a giant boulder, break a seawall, or tear out a building.

## IN CONCLUSION: TOWARD A NEW AWARENESS OF EXTREME COASTAL WAVE BEHAVIOUR

Amplification of wave height and onshore flow velocity should be taken into account when trying to determine upper limits of storm energy. Maximal waves with extreme onshore flow velocities will be rare events. But in considering whether boulders could be storm-transported, the possibility of extreme wave events—however statistically unlikely—cannot be discarded, and must be actively considered. This is especially true both for interpreting ancient deposits, and for coastal forward planning.

But onshore damage does not necessarily require the largest possible waves and the maximum possible velocities. Lesser waves—still larger than  $H_s$  or even  $H_{max}$  of a spectrum—may occur with greater frequency than the maximal monsters of Equation (8). The bottom line is that when considering storm-damage probabilities, and wave-coast interactions in general, waves with excess height and excess onshore velocity relative to offshore wave heights must be expected.

This analysis is rough, but the roughness is actually part of its value. It shines a light on an important truth: the equations are imprecise by necessity, because basic information is lacking. We hope that by unpacking the processes and exposing how poorly quantified they are, we can spur further research into the upper limits of onshore wave heights and onshore flows. As necessary data are gathered and understanding grows, better constraints and more robust values will be generated. In addition, every location is different, and so people applying this approach to specific sites should carefully consider the best local estimates for these variables. And we emphasise that we are not predicting wave heights and bore velocities for specific storms, but adopting a probabilistic method for evaluating possible extreme wave impacts over long time periods.

## DATA AVAILABILITY STATEMENT

All datasets generated for this study are included in the article.

## AUTHOR CONTRIBUTIONS

NB wrote the initial draft. NB and RC collaboratively wrote and revised the current paper.

## FUNDING

NB thanks the Ministry of Science and Technology of Taiwan for financial support [grant number 106-2911-I-006-301]. RC acknowledges support from National Science Foundation award 1529756.



## ACKNOWLEDGMENTS

We are grateful to reviewers Pedro J. M. Costa and A. B. M. Khan Mozahedy, whose critiques improved the manuscript,

and to Nobuhisa Kobayashi, James Herterich, and Andrew Kennedy for their insightful comments. Thanks also to Robb Tarr (<http://www.robtarr.co.za/>) for allowing us to use the photograph in **Figure 1**.

## REFERENCES

- Akrish, G., Rabinovitch, O., and Agnon, Y. (2016). Extreme run-up events on a vertical wall due to nonlinear evolution of incident wave groups. *J. Fluid Mech.* 797, 644–664. doi: 10.1017/jfm.2016.283
- Ardhuin, F., O'Reilly, W. C., Herbers, T. H. C., and Jessen, P. F. (2003). Swell Transformation across the Continental Shelf. Part I: attenuation and directional broadening. *J. Phys. Oceanogr.* 33, 1921–1939. doi: 10.1175/1520-0485(2003)033<1921:STATCS>2.0.CO;2
- Barbano, M. S., Pirrotta, C., and Gerardi, F. (2010). Large boulders along the south-eastern Ionian coast of Sicily: storm or tsunami deposits? *Mar. Geol.* 275, 140–154. doi: 10.1016/j.margeo.2010.05.005
- Benner, R., Browne, T., Brückner, H., Kelletat, D., and Scheffers, A. (2010). Boulder transport by waves: progress in physical modelling. *Z. Geomorphol. Suppl. Issues* 54, 127–146. doi: 10.1127/0372-8854/2010/0054S3-0022
- Boulton, S. J., and Whitworth, M. R. Z. (2017). Block and boulder accumulations on the southern coast of Crete (Greece): evidence for the 365 CE tsunami in the Eastern Mediterranean. *Geol. Soc. Lond. Spec. Publ.* 456:SP456.4. doi: 10.1144/SP456.4
- Bredmose, H., Bullock, G. N., and Hogg, A. J. (2015). Violent breaking wave impacts. Part 3. Effects of scale and aeration. *J. Fluid Mech.* 765, 82–113. doi: 10.1017/jfm.2014.692
- Brevik, Ø., Alves, J. H., Greenslade, D., Horsburgh, K., and Swail, V. (2017). The 14th international workshop on wave hindcasting and forecasting and the 5th coastal hazards symposium. *Ocean Dyn.* 67, 551–556. doi: 10.1007/s10236-017-1033-8
- Brennan, J., Clancy, C., Harrington, J., Cox, R., and Dias, F. (2017). Analysis of the pressure at a vertical barrier due to extreme wave run-up over variable bathymetry. *Theor. Appl. Mech. Lett.* 7, 269–275. doi: 10.1016/j.taml.2017.1.001
- Brill, D., May, S. M., Mhammedi, N., King, G., Burow, C., Wolf, D., et al. (2020). “OSL rock surface exposure dating as a novel approach for reconstructing transport histories of coastal boulders over decadal to centennial timescales,” in *EGU General Assembly, EGU2020-18537*. doi: 10.5194/egusphere-egu2020-18537
- Carbone, F., Dutykh, D., Dudley, J. M., and Dias, F. (2013). Extreme wave runup on a vertical cliff. *Geophys. Res. Lett.* 40, 3138–3143. doi: 10.1002/grl.50637
- Carrasco, A. R., Reis, M. T., Neves, M. G., Ferreira, Ó., Matias, A., and Almeida, S. (2014). Overtopping hazard on a rubble mound breakwater. *J. Coast. Res.* 70, 247–252. doi: 10.2112/SI70-042.1
- Cattrell, A. D., Srokosz, M., Moat, B. I., and Marsh, R. (2018). Can rogue waves be predicted using characteristic wave parameters? *J. Geophys. Res. Oceans* 123, 5624–5636. doi: 10.1029/2018JC013958
- Chang, K.-A., Ariyaratne, K., and Mercier, R. (2011). Three-dimensional green water velocity on a model structure. *Exp. Fluids* 51, 327–345. doi: 10.1007/s00348-011-1051-0
- Chanson, H. (2006). Tsunami surges on dry coastal plains: application of dam break wave equations. *Coast. Eng. J.* 48, 355–370. doi: 10.1142/S0578563406001477
- Chen, S. S., and Curcic, M. (2016). Ocean surface waves in Hurricane Ike (2008) and superstorm sandy, coupled model predictions and observations. *Ocean Model.* 103, 161–176. doi: 10.1016/j.ocemod.2015.08.005
- Chuang, W.-L., Chang, K.-A., and Mercier, R. (2015). Green water velocity due to breaking wave impingement on a tension leg platform. *Exp. Fluids* 56:139. doi: 10.1007/s00348-015-2010-y
- Cooker, M. J., and Peregrine, D. H. (1992). “Violent motion as near breaking waves meet a vertical wall,” in *Breaking Waves, International Union of Theoretical and Applied Mechanics*, eds M. L. Banner and R. H. J. Grimshaw (Berlin; Heidelberg: Springer), 291–297. doi: 10.1007/978-3-642-84847-6\_32
- Costa, P. J. M., Andrade, C., Freitas, M. C., Oliveira, M. A., da Silva, C. M., Omira, R., et al. (2011). Boulder deposition during major tsunami events. *Earth Surf. Process. Landf.* 36, 2054–2068. doi: 10.1002/esp.2228
- Cox, D. T., and Ortega, J. A. (2002). Laboratory observations of green water overtopping a fixed deck. *Ocean Eng.* 29, 1827–1840. doi: 10.1016/S0029-8018(02)00011-2
- Cox, R. (2019). Very large boulders were moved by storm waves on the west coast of Ireland in winter 2013–2014. *Mar. Geol.* 412, 217–219. doi: 10.1016/j.margeo.2018.07.016
- Cox, R., Ardhuin, F., Dias, F., Autret, R., Beisiegel, N., Earlie, C. S., et al. (2020). Systematic review shows that work done by storm waves can be misinterpreted as tsunami-related because commonly used hydrodynamic equations are flawed. *Front. Mar. Sci.* 7:4. doi: 10.3389/fmars.2020.00004
- Cox, R., Jahn, K. L., Watkins, O. G., and Cox, P. (2018). Extraordinary boulder transport by storm waves (west of Ireland, winter 2013–2014), and criteria for analysing coastal boulder deposits. *Earth Sci. Rev.* 177, 623–636. doi: 10.1016/j.earscirev.2017.12.014
- Denny, M. W., Miller, L. P., Stokes, M. D., Hunt, L. J. H., and Helmuth, B. S. T. (2003). Extreme water velocities: topographical amplification of wave-induced flow in the surf zone of rocky shores. *Limnol. Oceanogr.* 48, 1–8. doi: 10.4319/lo.2003.48.1.0001
- Didenkulova, I., and Anderson, C. (2010). Freak waves of different types in the coastal zone of the Baltic Sea. *Nat. Hazards Earth Syst. Sci.* 10, 2021–2029. doi: 10.5194/nhess-10-2021-2010
- Didenkulova, I., and Pelinovsky, E. (2011). Rogue waves in nonlinear hyperbolic systems (shallow-water framework). *Nonlinearity* 24, R1–R18. doi: 10.1088/0951-7715/24/3/R01
- Didenkulova, I. I., Slunyaev, A. V., Pelinovsky, E. N., and Kharif, C. (2006). Freak waves in 2005. *Nat. Hazards Earth Syst. Sci.* 6, 1007–1015. doi: 10.5194/nhess-6-1007-2006
- Dotet, G., Leckler, F., Sous, D., Ardhuin, F., Filipot, J., and Suanes, S. (2018). Wave runup over steep rocky cliffs. *J. Geophys. Res. Oceans* 123, 7185–7205. doi: 10.1029/2018JC013967
- Donnelly, C. (2008). *Coastal overwash: processes and modeling* (Ph.D. dissertation), Lund University, Lund, Sweden.
- Engel, M., and May, S. M. (2012). Bonaire’s boulder fields revisited: evidence for Holocene tsunami impact on the Leeward Antilles. *Q. Sci. Rev.* 54, 126–141. doi: 10.1016/j.quascirev.2011.12.011
- Esteban, M., Valenzuela, V. P., Matsumaru, R., Mikami, T., Shibayama, T., Takagi, H., et al. (2016). Storm surge awareness in the philippines prior to typhoon Haiyan: a comparative analysis with tsunami awareness in recent times. *Coast. Eng. J.* 58:1640009. doi: 10.1142/S057856341640009X
- Gemmrich, J., and Thomson, J. (2017). Observations of the shape and group dynamics of rogue waves: shape and group dynamics of rogue waves. *Geophys. Res. Lett.* 44, 1823–1830. doi: 10.1002/2016GL072398
- Hansom, J. D., Barltrop, N. D. P., and Hall, A. M. (2008). Modelling the processes of cliff-top erosion and deposition under extreme storm waves. *Mar. Geol.* 253, 36–50. doi: 10.1016/j.margeo.2008.02.015
- Herterich, J., Cox, R., and Dias, F. (2018). How does wave impact generate large boulders? Modelling hydraulic fracture of cliffs and shore platforms. *Mar. Geol.* 399, 34–46. doi: 10.1016/j.margeo.2018.01.003
- Herterich, J. G., and Dias, F. (2017a). Wave breaking and runup of long waves approaching a cliff over a variable bathymetry. *Proc. IUTAM* 25, 18–27. doi: 10.1016/j.piutam.2017.09.004
- Herterich, J. G., and Dias, F. (2017b). “Wave height to depth measures during extreme runup,” in *The 27th International Ocean and Polar Engineering Conference* (San Francisco, CA: International Society of Offshore and Polar Engineers), 1390–1394.
- Herterich, J. G., and Dias, F. (2019). Extreme long waves over a varying bathymetry. *J. Fluid Mech.* 878, 481–501. doi: 10.1017/jfm.2019.618



- Holland, K. T., Holman, R. A., and Sallenger, A. H. (1991). "Estimation of overwash bore velocities using video techniques," in *Coastal Sediments '91. Proceedings of a Speciality Conference on Quantitative Approaches to Coastal Sediment Processes*, Vol. 1 (Seattle, WA).
- Hu, Z., Xue, H., Tang, W., and Zhang, X. (2015). A combined wave-dam-breaking model for rogue wave overtopping. *Ocean Eng.* 104, 77–88. doi: 10.1016/j.oceaneng.2015.05.009
- Imamura, F., Goto, K., and Ohkubo, S. (2008). A numerical model for the transport of a boulder by tsunami. *J. Geophys. Res. Oceans* 113, 1–12. doi: 10.1029/2007JC004170
- Janjić, J., Gallagher, S., and Dias, F. (2018). Case study of the winter 2013/2014 extreme wave events off the west coast of Ireland. *Adv. Sci. Res.* 15, 145–157. doi: 10.5194/asr-15-145-2018
- Kennedy, A. B., Mori, N., Yasuda, T., Shimozone, T., Tomiczek, T., Donahue, A., et al. (2017). Extreme block and boulder transport along a cliffed coastline (Calicoan Island, Philippines) during Super Typhoon Haiyan. *Mar. Geol.* 383, 65–77. doi: 10.1016/j.margeo.2016.11.004
- Kennedy, A. B., Mori, N., Zhang, Y., Yasuda, T., Chen, S.-E., Tajima, Y., et al. (2016). Observations and modeling of coastal boulder transport and loading during super typhoon Haiyan. *Coast. Eng. J.* 58, 1640004-1–1640004-25. doi: 10.1142/S0578563416400040
- Kennedy, D. M., Tannock, K. L., Crozier, M. J., and Rieser, U. (2007). Boulders of MIS 5 age deposited by a tsunami on the coast of Otago, New Zealand. *Sediment. Geol.* 200, 222–231. doi: 10.1016/j.sedgeo.2007.01.005
- Kennedy, D. M., Woods, J. L. D., Naylor, L. A., Hansom, J. D., and Rosser, N. J. (2019). Intertidal boulder-based wave hindcasting can underestimate wave size: evidence from Yorkshire, UK. *Mar. Geol.* 411, 98–106. doi: 10.1016/j.margeo.2019.02.002
- Khariif, C., and Pelinovsky, E. (2003). Physical mechanisms of the rogue wave phenomenon. *Eur. J. Mech.* 22, 603–634. doi: 10.1016/j.euromechflu.2003.09.002
- Komar, P. D., and Allan, J. C. (2007). Higher waves along U.S. East Coast linked to hurricanes. *EOS Trans. Am. Geophys. Union* 88, 301–301. doi: 10.1029/2007EO300001
- Krogstad, H. E. (1985). Height and period distributions of extreme waves. *Appl. Ocean Res.* 7, 158–165. doi: 10.1016/0141-1187(85)90008-2
- Lorang, M. S. (2011). A wave-competence approach to distinguish between boulder and megaclast deposits due to storm waves versus tsunamis. *Mar. Geol.* 283, 90–97. doi: 10.1016/j.margeo.2010.10.005
- Lugni, C., Brocchini, M., and Falinsen, O. M. (2006). Wave impact loads: the role of the flip-through. *Phys. Fluids* 18:122101. doi: 10.1063/1.2399077
- Masselink, G., Scott, T., Poate, T., Russell, P., Davidson, M., and Conley, D. (2016). The extreme 2013/2014 winter storms: hydrodynamic forcing and coastal response along the southwest coast of England. *Earth Surf. Process. Landf.* 41, 378–391. doi: 10.1002/esp.3836
- Mastronuzzi, G., Pignatelli, C., Sansó, P., and Selli, G. (2007). Boulder accumulations produced by the 20th of February, 1743 tsunami along the coast of southeastern Salento (Apulia region, Italy). *Mar. Geol.* 242, 191–205. doi: 10.1016/j.margeo.2006.10.025
- Matias, A., Blenkinsopp, C. E., and Masselink, G. (2014). Detailed investigation of overwash on a gravel barrier. *Mar. Geol.* 350, 27–38. doi: 10.1016/j.margeo.2014.01.009
- Matias, A., Masselink, G., Castelle, B., Blenkinsopp, C. E., and Kroon, A. (2016). Measurements of morphodynamic and hydrodynamic overwash processes in a large-scale wave flume. *Coast. Eng.* 113, 33–46. doi: 10.1016/j.coastaleng.2015.08.005
- Matsutomi, H., and Okamoto, K. (2010). Inundation flow velocity of tsunami on land. *Island Arc* 19, 443–457. doi: 10.1111/j.1440-1738.2010.00725.x
- May, S. M., Engel, M., Brill, D., Cuadra, C., Lagmay, A. M. F., Santiago, J., et al. (2015). Block and boulder transport in Eastern Samar (Philippines) during Supertyphoon Haiyan. *Earth Surf. Dyn.* 3, 543–558. doi: 10.5194/esurf-3-543-2015
- Mentaschi, L., Voudoukas, M. I., Voukouvalas, E., Dosio, A., and Feyen, L. (2017). Global changes of extreme coastal wave energy fluxes triggered by intensified teleconnection patterns: global changes of extreme coastal waves. *Geophys. Res. Lett.* 44, 2416–2426. doi: 10.1002/2016GL072488
- Mottershead, D., Bray, M., Soar, P., and Farres, P. J. (2014). Extreme wave events in the central Mediterranean: geomorphic evidence of tsunami on the Maltese Islands. *Z. Geomorphol.* 58, 385–411. doi: 10.1127/0372-8854/2014/0129
- Nandasena, N. A. K., Paris, R., and Tanaka, N. (2011). Reassessment of hydrodynamic equations: Minimum flow velocity to initiate boulder transport by high energy events (storms, tsunamis). *Mar. Geol.* 281, 70–84. doi: 10.1016/j.margeo.2011.02.005
- Noormets, R., Crook, K. A. W., and Felton, E. A. (2004). Sedimentology of rocky shorelines: 3: hydrodynamics of megaclast emplacement and transport on a shore platform, Oahu, Hawaii. *Sediment. Geol.* 172, 41–65. doi: 10.1016/S0037-0738(04)00235-0
- Nott, J. (1997). Extremely high-energy wave deposits inside the Great Barrier Reef, Australia: determining the cause—tsunami or tropical cyclone. *Mar. Geol.* 141, 193–207. doi: 10.1016/S0025-3227(97)00063-7
- Nott, J. (2003a). Tsunami or storm waves? Determining the origin of a spectacular field of wave emplaced boulders using numerical storm surge and wave models and hydrodynamic transport equations. *J. Coast. Res.* 19, 348–356.
- Nott, J. (2003b). Waves, coastal boulder deposits and the importance of the pre-transport setting. *Earth Planet. Sci. Lett.* 210, 269–276. doi: 10.1016/S0012-821X(03)00104-3
- Ogawa, H., Dickson, M. E., and Kench, P. S. (2015). Hydrodynamic constraints and storm wave characteristics on a sub-horizontal shore platform. *Earth Surf. Process. Landf.* 40, 65–77. doi: 10.1002/esp.3619
- Park, H., Do, T., Tomiczek, T., Cox, D. T., and van de Lindt, J. W. (2018). Numerical modeling of non-breaking, impulsive breaking, and broken wave interaction with elevated coastal structures: laboratory validation and inter-model comparisons. *Ocean Eng.* 158, 78–98. doi: 10.1016/j.oceaneng.2018.03.088
- Peregrine, D. H. (2003). Water-wave impact on walls. *Annu. Rev. Fluid Mech.* 35, 23–43. doi: 10.1146/annurev.fluid.35.101101.161153
- Pignatelli, C., Sansó, P., and Mastronuzzi, G. (2009). Evaluation of tsunami flooding using geomorphologic evidence. *Mar. Geol.* 260, 6–18. doi: 10.1016/j.margeo.2009.01.002
- Poate, T., Masselink, G., Austin, M. J., Dickson, M., and McCall, R. (2018). The role of bed roughness in wave transformation across sloping rock shore platforms. *J. Geophys. Res. Earth Surf.* 123, 97–123. doi: 10.1002/2017JF004277
- Ritter, A. (1892). Die Fortpflanzung der Wasserwellen. *Z. Ver. Deutsch. Ingen.* 36, 947–954.
- Rixhon, G., May, S. M., Engel, M., Mechernich, S., Schroeder-Ritzrau, A., Frank, N., et al. (2018). Multiple dating approach (14C, 230Th/U and 36Cl) of tsunami-transported reef-top boulders on Bonaire (Leeward Antilles)—current achievements and challenges. *Mar. Geol.* 396, 100–113. doi: 10.1016/j.margeo.2017.03.007
- Roig-Munar, F. X., Rodríguez-Perea, A., Martín-Prieto, J. A., Gelabert, B., and Vilaplana, J. M. (2019a). Tsunami boulders on the rocky coasts of Ibiza and Formentera (Balearic Islands). *J. Mar. Sci. Eng.* 7:327. doi: 10.3390/jmse7100327
- Roig-Munar, F. X., Rodríguez-Perea, A., Vilaplana, J. M., Martín-Prieto, J. A., and Gelabert, B. (2019b). Tsunami boulders in Majorca Island (Balearic Islands, Spain). *Geomorphology* 334, 76–90. doi: 10.1016/j.geomorph.2019.02.012
- Roig-Munar, F. X., Vilaplana, J. M., Rodríguez-Perea, A., Martín-Prieto, J. A., and Gelabert, B. (2018). Tsunami boulders on the rocky shores of Minorca (Balearic Islands). *Nat. Hazards Earth Syst. Sci.* 18, 1985–1998. doi: 10.5194/nhess-18-1985-2018
- Ryu, Y., Chang, K.-A., and Mercier, R. (2007). Application of dam-break flow to green water prediction. *Appl. Ocean Res.* 29, 128–136. doi: 10.1016/j.apor.2007.10.002
- Scheffers, A. M., and Kinis, S. (2014). Stable imbrication and delicate/unstable settings in coastal boulder deposits: indicators for tsunami dislocation? *Q. Int.* 332, 73–84. doi: 10.1016/j.quaint.2014.03.004
- Scicchitano, G., Monaco, C., and Tortorici, L. (2007). Large boulder deposits by tsunami waves along the Ionian coast of south-eastern Sicily (Italy). *Mar. Geol.* 238, 75–91. doi: 10.1016/j.margeo.2006.12.005
- Shah-hosseini, M., Morhange, C., De Marco, A., Wante, J., Anthony, E., Sabatier, F., et al. (2013). Coastal boulders in Martigues, French Mediterranean: evidence for extreme storm waves during the Little Ice Age. *Z. Geomorphol.* 57, 181–199. doi: 10.1127/0372-8854/2013/S-00132

- Shah-hosseini, M., Morhange, C., Naderi Beni, A., Marriner, N., Lahijani, H., Hamzeh, M., et al. (2011). Coastal boulders as evidence for high-energy waves on the Iranian coast of Makran. *Mar. Geol.* 290, 17–28. doi: 10.1016/j.margeo.2011.10.003
- Slunyaev, A., Didenkulova, I., and Pelinovsky, E. (2011). Rogue waters. *Contemp. Phys.* 52, 571–590. doi: 10.1080/00107514.2011.613256
- Song, Y. K., Chang, K.-A., Ariyaratne, K., and Mercier, R. (2015). Surface velocity and impact pressure of green water flow on a fixed model structure in a large wave basin. *Ocean Eng.* 104, 40–51. doi: 10.1016/j.oceaneng.2015.04.085
- Switzer, A. D., and Burston, J. M. (2010). Competing mechanisms for boulder deposition on the southeast Australian coast. *Geomorphology* 114, 42–54. doi: 10.1016/j.geomorph.2009.02.009
- Switzer, A. D., Yu, F., Gouramanis, C., Soria, J. L. A., and Pham, D. T. (2014). Integrating different records to assess coastal hazards at multi-century timescales. *J. Coast. Res.* 70, 723–729. doi: 10.2112/SI70-122.1
- Viotti, C., and Dias, F. (2014). Extreme waves induced by strong depth transitions: Fully nonlinear results. *Phys. Fluids* 26:051705. doi: 10.1063/1.4880659
- Weiss, R., and Diplas, P. (2015). Untangling boulder dislodgement in storms and tsunamis: is it possible with simple theories? *Geochem. Geophys. Geosyst.* 16, 890–898. doi: 10.1002/2014GC005682
- Weiss, R., and Sheremet, A. (2017). Toward a new paradigm for boulder dislodgement during storms. *Geochem. Geophys. Geosyst.* 18, 2717–2726. doi: 10.1002/2017GC006926
- Wüthrich, D., Pfister, M., Nistor, I., and Schleiss, A. J. (2018). Experimental study of tsunami-like waves generated with a vertical release technique on dry and wet beds. *J. Waterway Port Coast. Ocean Eng.* 144:04018006. doi: 10.1061/(ASCE)WW.1943-5460.0000447
- Yeh, H., Liu, P., Briggs, M., and Synolakis, C. (1994). Propagation and amplification of tsunamis at coastal boundaries. *Nature* 372, 353–355. doi: 10.1038/372353a0
- Yeh, H. H. (1991). “Tsunami bore runup,” in *Tsunami Hazard: A Practical Guide for Tsunami Hazard Reduction*, ed E. N. Bernard (Dordrecht: Springer Netherlands), 209–220. doi: 10.1007/978-94-011-3362-3\_7
- Zainali, A., and Weiss, R. (2015). Boulder dislodgement and transport by solitary waves: insights from three-dimensional numerical simulations. *Geophys. Res. Lett.* 42:2015GL063712. doi: 10.1002/2015GL063712
- Zhang, Y., Kennedy, A. B., Tomiczek, T., Yang, W., Liu, W., and Westerink, J. J. (2017). Assessment of hydrodynamic competence in extreme marine events through application of Boussinesq–Green–Naghdi models. *Appl. Ocean Res.* 67, 136–147. doi: 10.1016/j.apor.2017.06.001

**Conflict of Interest:** The authors declare that the research was conducted in the absence of any commercial or financial relationships that could be construed as a potential conflict of interest.

Copyright © 2020 Bujan and Cox. This is an open-access article distributed under the terms of the Creative Commons Attribution License (CC BY). The use, distribution or reproduction in other forums is permitted, provided the original author(s) and the copyright owner(s) are credited and that the original publication in this journal is cited, in accordance with accepted academic practice. No use, distribution or reproduction is permitted which does not comply with these terms.